Feasibility of Rotating Fluidized Bed Reactor for Rocket Propulsion

HANS LUDEWIG, A. JAMES MANNING, AND CHAD J. RASEMAN
Brookhaven National Laboratory, Upton, N.Y.

The rotating fluidized bed reactor concept is outlined and its application to rocket propulsion discussed. Experimental results obtained indicate that minimum fluidization correlations commonly in use for 1-g beds can also be applied to multiple-g beds. It was found that for a low thrust system [90,000N (20,000 lbf)] the fuel particle size and/or particle stress play a limiting role on performance. The superiority of ^{233}U as a fuel for this type of rocket engine is clearly demonstrated in the analysis. The maximum thrust/weight ratio for a 90,000N thrust engine was found to be approximately 65N/kg.

Introduction

THE rotating fluidized bed reactor concept was initially proposed as a propulsion reactor in 1960.[1,2] A schematic representation of such a rocket engine is shown in Fig. 1. Fuel (UC-ZrC) in the form of small diameter particles (100–500μ in diam) is retained by centrifugal force in a rotating cylindrical structure to form an annular core. The cylinder is made up of a porous material backed up by a squirrel cage-type support structure known as a frit. Hydrogen propellant passes first through the cooling passages in the rocket nozzle and then through the reflector. All or part of it then passes through the turbine of the turbo-pump unit and then enters the core region. The gas flows radially inward through the cylindrical structure and annular core at a velocity sufficient to fluidize most of the bed. Finally, the heated gas flows out through the nozzle generating the desired thrust. The advantages of such a concept over other nuclear propulsion systems have been outlined in Ref. 2, and will be summarized here.

1) The larger surface-to-volume ratio of the fuel and the high fuel-to-coolant heat transfer coefficients permits very high rates of heat transfer with minimum temperature difference between the fuel and gas streams.

2) Since the primary structure remains cool, design requirements are dictated by the high temperature stability of the fuel rather than structural factors which are limiting in conventional solid fuel element nuclear propulsion system.

3) The volume and mass of material that must be handled in loading and unloading fuel is less than that handled in comparable solid fuel element systems and refueling of the core is simplified.

4) The fuel particles are retained in the core by centrifugal forces and the fuel loss problems that are characteristic of gas core concepts are minimized.

It is the purpose of this article to outline the latest experimental data obtained on a new bed, correct the previously made critical mass estimates[2] and analyze the performance of the rocket engine in a more complete manner. Experiments were designed to extend the data into regions which would be more compatible with propulsion reactors. Analytically derived results cover both the reactor physics parameters, such as critical uranium loading, and engineering quantities such as temperature distribution within the fuel bed. The latter quantities are related to an engine of a specific thrust.

Experimental Methods and Results

These experiments were designed to: a) study the bed dynamics and b) obtain an experimental correlation which can be used to predict the point of minimum fluidization, i.e., the minimum flow rate required to fluidize a given bed.

The current experimental program differs from that carried out earlier[3] in that the bed length and diameter are equal [25.4 cm (10 in.)]. In the previous case, the length-to-diameter was 0.1;

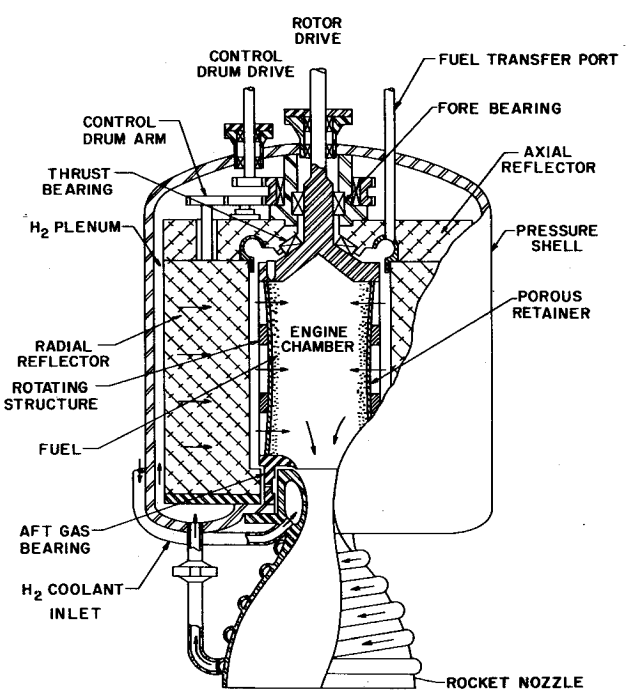

Fig. 1 Schematic diagram of a rotating fluidized bed rocket engine.

Received July 9, 1973; revision received October 3, 1973. This work was performed under the auspices of the Space Nuclear Systems Office, a joint office of the USAEC and NASA Agreement 13254. The authors wish to thank C. E. Franklin, D. J. Miller, and N. Gerstein of the Space Nuclear Systems Office, U.S. Atomic Energy Commission for their support. Thanks are also due to J. M. Hendrie, the late J. Chernick, M. M. Levine, and K. C. Hoffman at Brookhaven National Laboratory for many helpful discussions regarding this work.

Index category: Nuclear Propulsion.

* Assistant Physicist.

† Process Engineer; presently at Celanese Research Corp., Summit, N.J.

‡ Chemical Engineer; presently at Solar Sunstill, Inc., Setauket, N.Y.

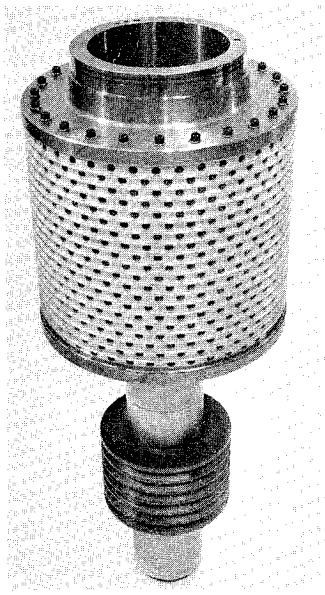

Fig. 2 Rotating drum showing perforated frit support, drive shaft, pulley, and nozzle.

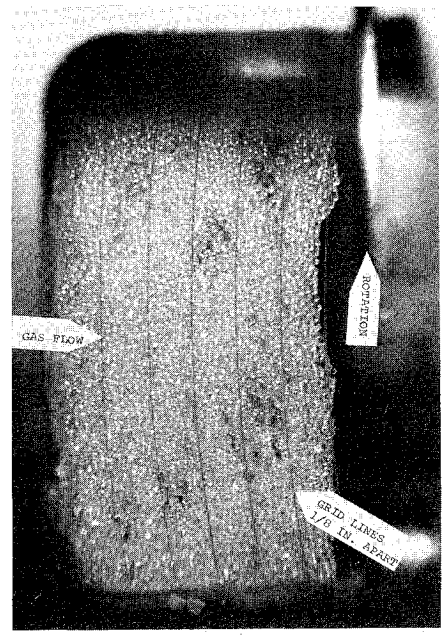

Fig. 4 View of bed taken through bottom plate, 500μ glass, 1000 rpm, 170 m^3/min.

the present experiments would make the bed geometry agree more closely with conceptual designs for a propulsion reactor. The experimental setup has been described in great detail elsewhere[4] and will briefly be described here.

High pressure nitrogen (gas used in the cold flow experiments) is supplied to the gas distribution shell after it has passed through a pressure regulator, an orifice to measure flow, and a flow control valve. Figure 2 is of the rotating drum showing the perforated frit support, drive shaft, pulley, and nozzle.

Bed Dynamics

Dynamic behavior of the bed was determined by using high-speed photographic techniques. The bed apparatus is arranged so that single frame photographs may be taken through windows in the bottom plate of the rotating assembly.

Two photographs of the bed in this experimental series are shown in Figs. 3 and 4. For experiments at 140 g (1000 rpm), flow rates were varied from 0–170 STP m^3/min (0–6000 SCFM). The settled bed (zero flow) is approximately 1.60 cm ($\frac{5}{8}$ in.) thick in this particular case and made up of 500μ glass spheres. It is seen that the bed expands to about 1.9 cm ($\frac{3}{4}$ in.) when the flow of gas reaches 170 STP m^3/min (6000 SCFM) and "bubbles" of gas are starting to form within the bed. It has been found that these gas bubbles can be eliminated by increasing the rotational speed.

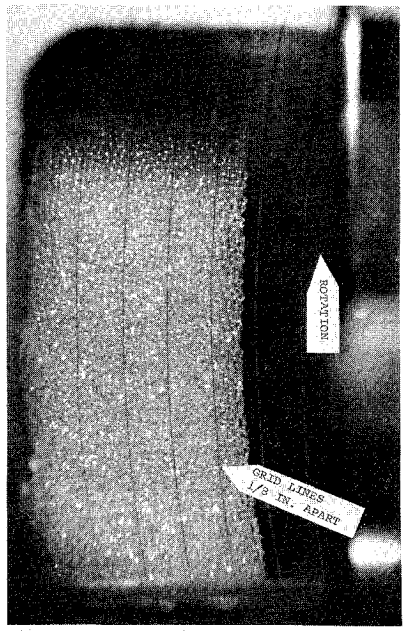

Fig. 3 View of bed taken through bottom plate, 500μ glass, 1000 rpm, 0 m^3/min.

Experimental data from the present series, together with that gathered from the previous experiment,[3] demonstrate that a rotating fluidized bed can be operated in a stable mode over a range of length diameter ratios of 0.1–1.0. Furthermore, to achieve a bed free from bubbles but maintaining a high flow rate, the rotating speed need only be increased, increasing the gravitational force. This is an important feature for reactor operations, since it would thus be possible to vary the power over a wide range. More specifically, in the case of rocket propulsion it would enable the same reactor to operate over a wide thrust range.

Minimum Fluidization

The point of minimum fluidization occurs when the drag forces on the bed due to the gas flow balances the weight of the bed. This condition is determined experimentally by measuring the pressure drop across the bed as a function of flow rate. Initially, the bed will be settled, and as the flow rate is increased, the pressure drop increases until the balance point is reached. After this point, the pressure drop across the bed stays constant with increasing flow rate.

Figure 5 shows typical variations of pressure drop as a function of flow rate. It can be seen that in all cases where the settled bed thickness was 0.95 cm ($\frac{3}{8}$ in.) a point of minimum fluidization was determined. In the case of the other bed thicknesses shown, a higher flow rate would be required to fluidize the bed.

It is interesting to note from the curves in Fig. 5 that at least two of the three cases reaching the minimum fluidization condition show a characteristic "hump." This "hump" indicates that a larger pressure drop than that required for fluidization occurs and has been attributed[5] to frictional forces occurring

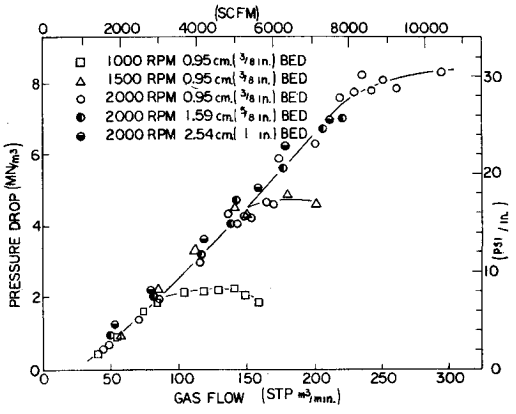

Fig. 5 Correlation of fluidization data for 500μ glass beads (specific gravity = 2.5).

within the bed. This phenomenon is most frequently seen in beds composed of small diameter particles, such as the ones under consideration.

Resulting from this experimental program is a correlation useful in predicting the point of minimum fluidization. This is an important piece of information since this would automatically give the minimum flow rate to fluidize a system which is dynamically similar. This correlation is obtained by plotting Galileo number (Ga) as a function of Reynolds number (Re) where

$$Ga = D_p{}^3\rho(\rho_p - \rho)g/\mu^2$$

and

$$Re = GD_p/\mu$$

ρ, μ, G = the fluid density, viscosity, and mass flow rate per unit area, respectively
D_p, ρ_p = the particle diameter and density
g = the gravitational acceleration

The correlation, which has been suggested[6] by earlier workers using 1.0 g beds, is

$$Re_{mf} = [(33.7)^2 + 0.0408 Ga_{mf}]^{1/2} - 33.7 \quad (1)$$

The subscript mf refers to minimum fluidization in the above equation.

Figure 6 shows Eq. (1) and the experimentally obtained results. It can be seen that the fit between Eq. (1) and experiment is good.

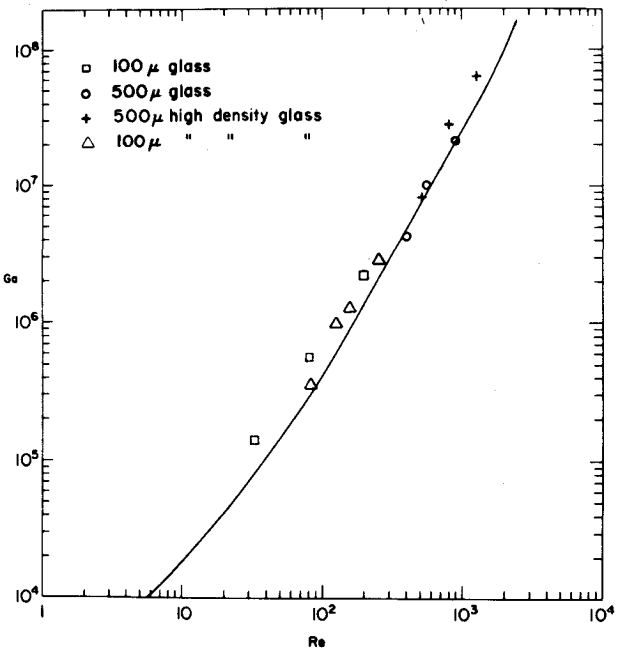

Fig. 6 Correlation of Galileo number vs Reynolds number for minimum fluidization.

Reactor Physics and Rocket Engine Operating Condition

In this section the reactor physics associated with this type of reactor and an analysis of the operating conditions of a rocket propulsion reactor based on this concept are outlined. Details of the critical mass determination are outlined next, to be followed by an analysis of the operating conditions of a 90,000 N (20,230 lbf) thrust rocket engine.

Critical Mass Determination

The critical mass determination was made using the two-dimensional representations shown in Fig. 7. However, before computations could be carried out using this representation, appropriate few-group cross sections had to be determined. Few-group cross sections were obtained by assuming a one-dimensional model with many energy groups. In this way, an accurate representation of the neutron energy spectrum can be determined in the various regions of the reactor, and can be used to collapse the large number of micro-groups to fewer macrogroups. Only a radial variation was allowed for in the one-dimensional model; thus, the cavity, fuel bed, frit and reflector were assumed to be coaxial cylinders. In this way, the spatial variation of the spectrum from the cavity containing hot hydrogen to the reflector composed of beryllium and hydrogen can be accounted for. Furthermore, the diffusion cooling effects in the spectrum, due to the neutron leakage out of the reflector are incorporated.

The one-dimensional calculations were further divided into two separate calculations, one for those neutrons above the thermal cutoff and another for those below the cutoff. In this case, the thermal cutoff was assumed to be 2.15 ev. The epithermal range was treated by using the ABBN[7] cross section set and the diffusion theory code 1-DX.[8] It was felt that diffusion theory would be adequate in this range since the flux gradients would not be very steep. Four few-group cross sections were obtained from these calculations for the epithermal range. In the thermal range a great deal of care had to be taken since the gradients in the neutron flux from the reflector into the fuel region are very steep, the Bragg scattering of beryllium had to be accounted for, and the reactor is highly thermal. For these

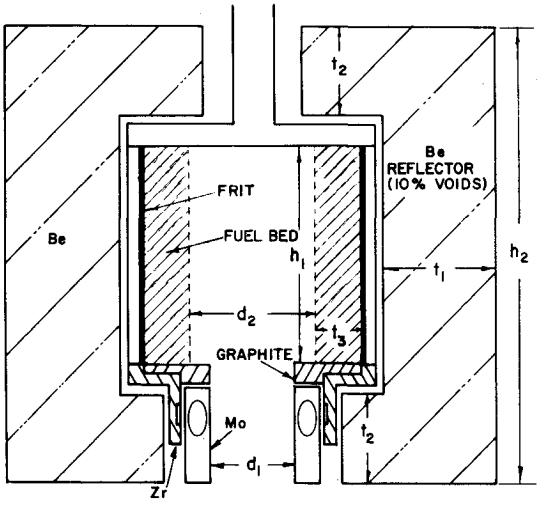

Fig. 7 Two-dimensional reactor model.

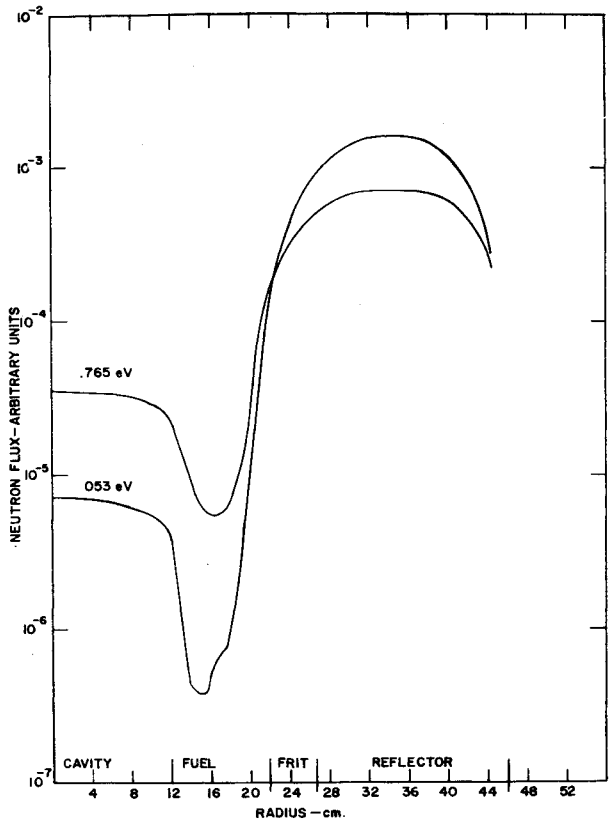

Fig. 8 Spatial variation of neutron flux.

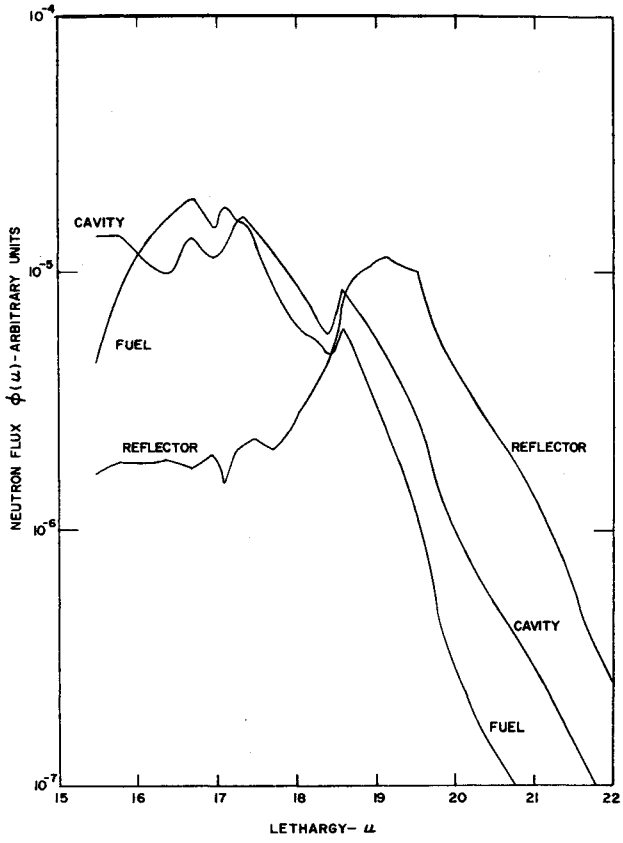

Fig. 9 Neutron spectra at various positions.

reasons, the one-dimensional calculations were carried out using 30 thermal groups, with up and down scattering among all groups and the DSN code ANISN.[9] These cross sections were based on ENDF/B data and collapsed down to a single macro-group in the thermal range.

Results of the one-dimensional calculation in the thermal range are shown in Figs. 8 and 9 for a ^{233}U fueled reactor. Figure 8 shows the spatial variation of the neutron flux for 0.765 and 0.053 ev. The discontinuity in the 0.053 ev curve occurs at the point where the bed changes from settled to fluidized. Figure 9 shows the neutron energy spectrum in the cavity, fuel and reflector. From these curves the progressive softening of the spectrum is evident as one moves out from the cavity to the reflector.

Criticality determinations of the actual rocket reactor were carried out using the two-dimensional DSN code DOT.[10] All the two-dimensional calculations were carried out using the five macro-group cross sections and four angular quadratures. As an example, the critical dimension for a ^{233}U-fueled reactor and a ^{235}U-fueled reactor are given in Table 1. Both these reactors are optimized around a thrust of 90,000 N (20,230 lbf).

Table 1 Critical dimension for 90,000 N thrust engine

	^{233}U Fueled reactor	^{235}U Fueled reactor
throat diam (d_1)	18 cm	18 cm
bed internal diam (d_2)	24 cm	48 cm
radial reflector thickness (t_1)	16 cm	21 cm
axial reflector thickness (t_2)	25 cm	25 cm
fuel bed thickness (t_3)	10 cm	10 cm
cavity height (h_1)	44 cm	74.7 cm
over-all height (h_2)	104 cm	135.0 cm
critical mass (m_1)	140.0 kg	420.0 kg

90,000 N Thrust Engine Operating Conditions

It has been found[11,12] from earlier investigations that the reflector weight dominates the total weight of the system and there is a great incentive to reduce the reflector weight. A reduction in reflector weight and hence thickness, increases the neutron leakage. The loss of neutrons may be compensated for by reducing the nozzle area and thus the loss due to streaming. However, a nozzle of reduced area implies a higher chamber pressure to maintain a desired thrust level. The increased chamber pressure increases the weight of the containment vessel and turbo-pump. Thus, it was found that a reduction in the reflector weight implied an increase in the weight of the remainder of the system and vice versa. An optimum throat area can be found which minimizes the weight for a given thrust level, thus maximizing the thrust/weight ratio.

An important component of the pressure to be overcome by the turbo-pump is the pressure drop across the fuel bed. It was found that the fuel particle size can, under certain circumstances, be a limiting factor on the optimum thrust/weight ratio of an engine. This limitation is brought about by the balance between low fuel bed pressure drops for large particle diameters and high thermal stress for large particle diameters.

The total weight of the system will be defined to be composed of: a) fixed weight (fuel, reflector, rotating gear); b) nozzle and controls; c) pressure vessel; and d) turbo-pump. Weights for the last three items are based on a model proposed by Johnson and Smith.[13] The fixed weight was determined by the criticality calculations. In estimating the weights for the last three items of the list above, it is necessary to know the pressure and temperature at various points within the propellant supply system. It was assumed that the propellant is pumped out of a supply tank and passes through a pump, nozzle, reflector, turbine and the fuel bed before entering the cavity. This path is shown schematically in Fig. 10. The model used for estimating the temperature rise T_1 to T_2 and pressure drop P_1 to P_2 was based on Ref. 14. Relationships between T_3P_3 and T_2P_2 can be

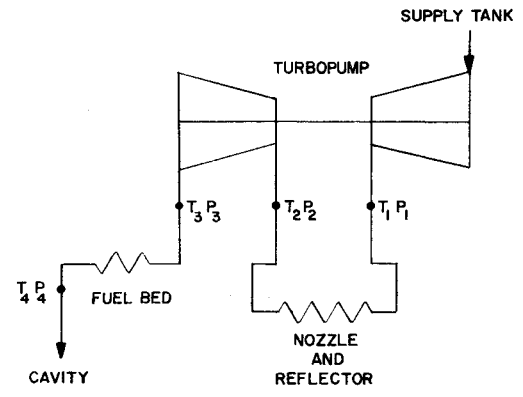

Fig. 10 Schematic of flow system.

obtained from the power requirements by the turbo-pump unit. The relationship between T_4P_4 and T_3P_3 is obtained from the model used for the fuel bed. In the remainder of this section the methods for computing the temperature shape within the fuel bed and the pressure drop will be outlined. Finally, the dependence of thrust/weight ratio on nozzle diameter, the implied variation of system weight mentioned above, and the fuel particle diameter will be discussed.

In estimating the variation within the bed of the gas and fuel particle temperature, the assumption will be made that the fuel bed can be represented by a homogeneous mixture. Thus, separate energy balance equations can be written for the solid (fuel particle) phase and gas phase.

The equations to be considered are

a) gas phase

$$h(T_g)A(1-\varepsilon)(T_s-T_g) = -G\nabla(C_p T_g) \tag{2}$$

b) solid phase

$$Q(\bar{r}) = h(T_g)A(1-\varepsilon)(T_s-T_g) - k_e\nabla^2 T_s \tag{3}$$

where

T_g = gas temperature
T_s = solid temperature (fuel particle surface)
A = fuel surface area
$h(T_g)$ = heat transfer coefficient
G = mass flow rate (per unit area)
C_p = specific heat at constant pressure
ε = bed void fraction
k_e = effective thermal diffusion coefficient
$Q(r)$ = imposed heat source.

The effect of including k_e in the determinations of the temperatures T_g and T_s has been estimated and found to be negligible ($\pm 0.4\%$). In the model for computing the variation of T_g and T_s, it was thus assumed that the conduction term in Eq. (3) can be neglected. Furthermore, the flow of propellant was assumed to be only radial, i.e., $G = \dot{m}/2\pi rh$, where $\dot{m}$ = total mass flow rate. The following equations can thus be written for the gas temperature and the solid (fuel particle surface) temperature.

$$(-d/dr)(C_p T_g) = (2\pi rh/\dot{m})Q(r, z) \tag{4}$$

and

$$T_s = T_g + [Q(r, z)/h(T_g)A(1-\varepsilon)] \tag{5}$$

The boundary conditions on these equations are: a) T_g (r = outer bed radius) = T_3 and b) the imposed heat source $Q(r, z)$ is normalized in such a fashion that at the inner bed surface the gas temperature in the cavity, T_4, reaches the level dictated by performance requirements. The shape of $Q(r, z)$ is obtained from the criticality calculations, and is given by the fission distribution within the fuel bed. The heat transfer coefficient, $h(T_g)$, can be computed from a correlation by Sen Grupta et al.[15] for the packed section of the bed, i.e.

$$Nu = 2.06/\varepsilon\, Re^{0.425}\, Pr^{1/3} \tag{6}$$

where Nu = Nusselt number and Pr = Prandtl number

In the fluidized section of the bed, the Nusselt number is essentially flow rate independent. This was hypothesized by Chang et al.[16] and demonstrated by Lindauer.[17] The correlation used in this region of the bed is given by[16]:

$$Nu = 2.0 + 0.79\, Ga^{1/4}\, Pr^{1/3} \tag{7}$$

Furthermore, the particle thermal stress is given by[18]:

$$\sigma = E\alpha Q(r, z)D_p^2/24K(1-v)$$

where

E = Young's modulus
α = coefficient of expansion
K = thermal diffusion coefficient from particles
v = Poisson's ratio

It is seen that the stress is directly proportional to the power, and particle diameter squared. Since this is a reflector moderated reactor, the highest power densities occur at the outer edges of the bed, where the particles would be at the lowest temperature. It is, thus, seen that the particles sustaining the highest stress are the coolest. Finally, the probability for a hot particle entering this region of high stress is remote, since this section of the bed will very likely be settled in an operating reactor.

The fuel bed was considered to be made up of two distinct regions, one fluidized and one settled. This assumption is supported by photographic evidence gathered from the experimental program. The bed fluidizes at the inside edge first, with the boundary between fluidized and settled region moving out with increasing flow rate at a given rotational speed; a model to simulate a two-region bed was used.

Using the experimentally confirmed correlation given by Eq. (1), it can be shown that

$$g = V_e X(D_p X + 67.4)/0.0408 D_p^3 Y \tag{9}$$

where

V_e = superficial velocity
$X = \rho/\mu$ = kinematic viscosity
$Y = (\rho_p - \rho)/\mu^2$

Thus, given the superficial velocity and a particle diameter, the gravitational force required for fluidization can be determined. Hence, the pressure drop across the fluidized section of the bed can be computed.

In the settled region the pressure drop is given by[19]

$$\Delta p = \left[\frac{150(1-\varepsilon)}{Re} + 1.75\right]\frac{LG^2(1-\varepsilon)}{D_p\varepsilon^3 32.17} \tag{10}$$

where

L = thickness of packed section.

The total pressure drop can thus be computed using Eqs. (9) and (10).

Using the model outlined above the temperature and pressure variations within the bed for a 90,000 N (20,230 lbf) thrust, ^{233}U-fueled rocket engine is shown in Fig. 11.

The above results apply to an engine having a specific impulse of 8185 m/sec (835 sec). However specific impulses to 9820 m/sec (1000 sec) are felt to be possible with this system.

From Eqs. (9) and (10) it can be seen that the total pressure drop increases with increasing V_e and decreasing D_p. In order to decrease V_e for a given reactor, the propellant flow rate has to be reduced; however, to maintain a constant thrust level, the cavity pressure must be increased. It is thus seen that the sum of the cavity pressure and the bed pressure drop must be minimized. In minimizing this combined pressure, it is important to take account of the corresponding particle diameter, since the bed pressure drop decreases with increasing particle size. Although this decrease is very desirable, increasing the particle size is not, since its thermal stress rises very rapidly.

The specific example to illustrate the type of results obtained from the above discussion will be a rocket reactor generating 90,000 N (20,230 lbf) of thrust and fueled by ^{233}U. A maximum

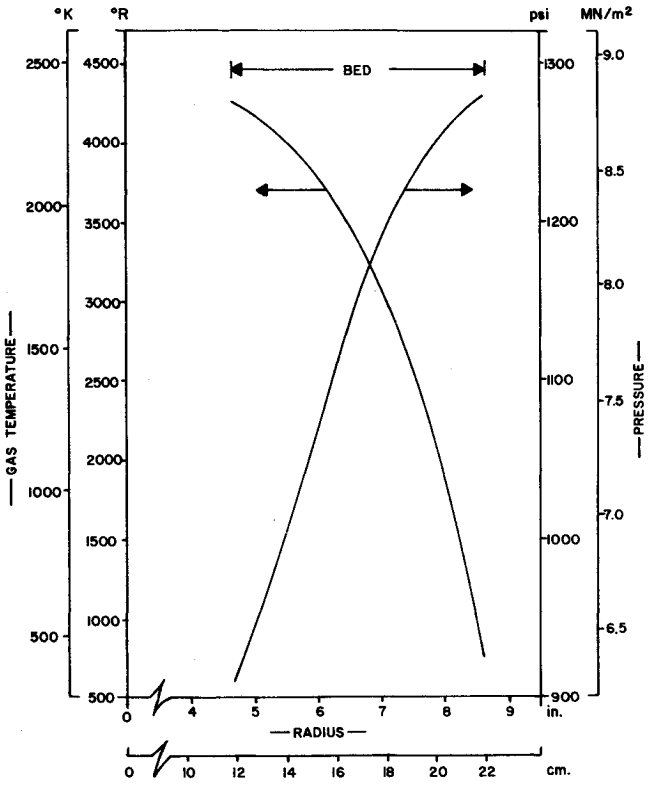

Fig. 11 Variation of pressure and temperature within bed for a 90,000 N thrust ^{233}U-fueled engine.

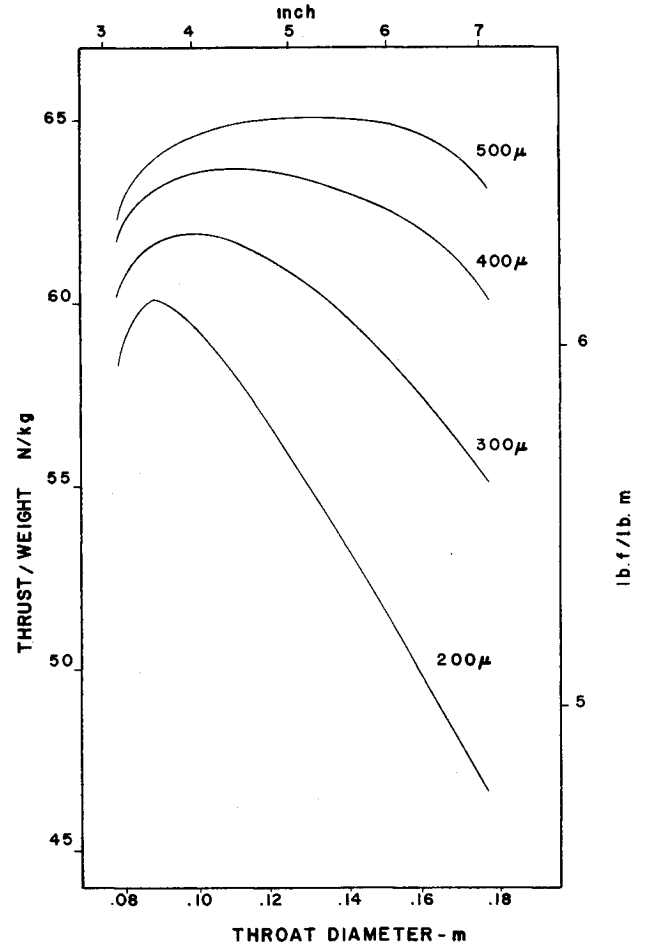

Fig. 12 Variation of thrust-to-weight ratio with nozzle diameter for selected fuel (^{233}U-fueled reactor).

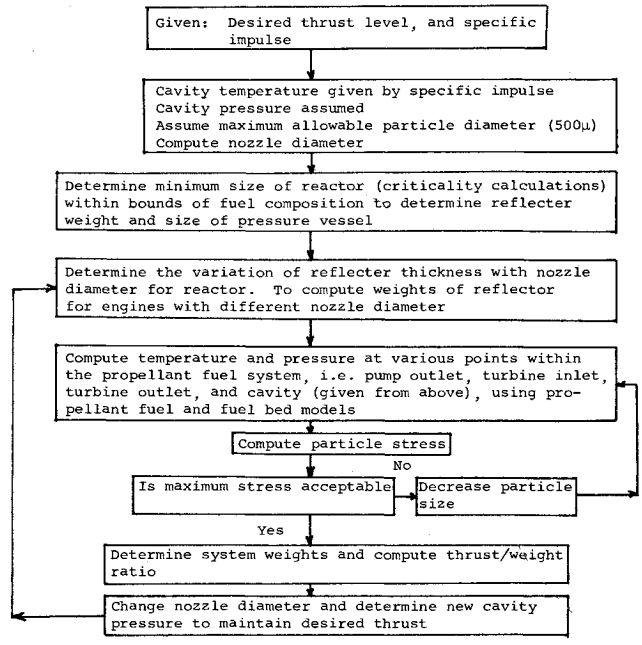

Fig. 13 Flow diagram for thrust/weight optimization.

particle diam of 500μ and/or a maximum thermal stress of 55 MN/m^2 (8000 psia) will also be assumed. The variation of thrust/weight ratio as a function of throat diameter and particle size is shown in Fig. 12 for this system. The curves on Fig. 12 include the optimization discussed above regarding the trade-off between reflector weight and the weight of the remainder of the system. However, they also include the effect of different particle size. Briefly, increasing the throat diameter improves the performance initially, due to a reduction in cavity pressure, which reduces the pump and pressure vessel weight. However, larger throat diameters require increasingly heavier reflectors which reduce the performance. Furthermore, it can be seen that larger fuel particle diameters correspond to improved performance levels since they result in lower fuel bed pressure drops.

It is interesting to note that for a combination fluidized-settled bed of this type, for a constant particle diameter, and constant thrust, the Reynolds number is constant. This implies a constant Galileo number; however, increasing the throat diameter decreases the cavity pressure and thus the propellant density. It is thus seen that g has to increase to maintain a constant Galileo number. Therefore, for the same reactor operating at a constant thrust the bed pressure drop will increase rapidly with increasing throat diameter. This explains, in part, the rapid drop off of the curves for 200μ and 300μ diam particles for the larger throat diameters in Fig. 12. For larger particle diameters the bed pressure drop is comparatively small and this effect is not important.

Finally, it can be seen from Fig. 12 that an engine using ^{233}U as a fuel can generate a thrust of 90,000 N (20,230 lbf) at a thrust/weight ratio of approximately 65 N/kg (6.63 lbf/lb m). At higher thrust levels it is possible to improve upon this performance, i.e. a ^{233}U fuel engine generating a thrust of 1.8×10^6N (400,000 lbf) could conceivably operate at a thrust/weight ratio of 167 N/kg (17.0 lbf/lb m). The method used for determining the maximum thrust/weight ratio is summarized in Fig. 13.

Summary and Conclusions

1) The experimental results obtained indicate that the rotating fluidized bed is a feasible concept operating satisfactorily over a wide range of parameters.

2) Experimental data obtained fits the minimum fluidization correlations used for 1-g beds (Fig. 6).

3) From the reactors studied, it is evident that although a rocket engine based on this concept would be able to operate over a large range of thrust, it is worthwhile to optimize it for a thrust range of interest.

4) In addition to problems posed by optimizing the reflector weight and the remainder of the system weight by adjusting the nozzle throat diameter, it has been found that the particle size and/or stress play a limiting role on performance (Fig. 12).

5) For comparatively low thrust rocket engines, ^{233}U seems to have an overwhelming advantage over ^{235}U-fueled engines from a performance point of view. This conclusion is based on a thrust/weight ratio of 65.7 N/kg (6.7 lbf/lb_m) for a ^{233}U-fueled engine and 33.3 N/kg (3.4 lbf/lb_m) for a ^{235}U-fueled engine. Both these engines produced 90,000 N of thrust, and had a specific impulse of 8185 m/sec (835 sec).

6) The small size of the fuel particles greatly reduces the difference between the gas temperature and the maximum fuel temperature. In the case of conventional reactors this difference could be an order of magnitude higher (Fig. 11).

7) A possibility for the continuous replacement of fuel exists in this concept, which would minimize fission product build-up and reduce the over-all fuel loading. The core excess reactivity would not have to be high at beginning of life.

References

[1] Hatch, L. P., Regan, W. H., and Powell, J. R., "Fluidized Solids as a Nuclear Fuel for Rocket Propulsion," ARS Semi-Annual Meeting, Los Angeles, Calif. (May 1960).

[2] Hatch, L. P., Regan, W. H., and Powell, J. R., "Fluidized Beds for Rocket Propulsion," *Nucleonics*, Vol. 18, No. 12, 1960, p. 102.

[3] Lindauer, G. C., Tichler, P., and Hatch, L. P., "Experimental Studies on High-Gravity Rotating Fluidized Beds," BNL-50013 (T-435), 1966, Brookhaven National Laboratory, Upton, N.Y.

[4] "Rotating Fluidized Bed Reactor for Space Nuclear Propulsion," *Annual Report. Design Studies and Experimental Results, June 1970–June 1971*, BNL-50321 (UC-33), Brookhaven National Lab., Upton, N.Y., 1971.

[5] Richardson, J. F., *Fluidization*, edited by J. F. Richardson and D. Harrison, Academic Press, N.Y., 1971, p. 26.

[6] Wen, C. Y. and Yu, Y. H., "Mechanics of Fluidization," *Chemical Engineering Progress Symposium Series*, No. 62, 1966, p. 100.

[7] Abagyn, et al., *Group Constants for Nuclear Reactor Calculations*, Consultants Bureau, New York, 1964.

[8] Hardie, R. W. et al., "1-DX, A One-Dimensional Diffusion Code for Generating Effective Nuclear Cross Sections," BNWL-854, 1969, Battelle Memorial Institute, Richland, Wash.

[9] Engle, W. W., "A User's Manual for ANISN, A One-Dimensional Discrete Ordinate Transport Code with Anisotropic Scattering," K-1693, Oak Ridge National Lab., Union Carbide Corp., Tenn.

[10] Mynatt, F. R., "A User's Manual for DOT," Rept. K-1694 (in press), Oak Ridge National Lab., Union Carbide Corp.

[11] Ludewig, H., "Design Parameters for a Rotating Bed Reactor Powered Rocket Engine," *Transactions of the American Nuclear Society*, Vol. 15, No. 1, 1972, p. 8.

[12] Ludewig, H. and Chernick, J., "Physics Parameters of the Hatch Reactor," *Transactions of the American Nuclear Society*, Vol. 14, No. 1, 1971, p. 11.

[13] Johnson, P. G. and Smith, R. L., "Optimization of Power Plant Parameters for Orbital-Launch Nuclear Rockets," TN-D-675, 1961, NASA.

[14] "Engineering Study of Colloid-Fueled Nuclear Rocket," ARL-69-0234, 1969, Aeronautical Research Lab., Wright-Patterson Air Force Base, Ohio.

[15] Sen Grupta, A. and Thodos, G., "Direct Analogy between Mass and Heat Transfer to Beds of Spheres," *American Institute of Chemical Engineers Journal*, Vol. 9, 1963, p. 751.

[16] Chang, T. M. and Wen, C. Y., "Fluid-to-Particle Heat Transfer in Air Fluidized Beds," Chemical Engineering Progress Symposium Series, Vol. 62, No. 67, 1966, p. 111.

[17] Lindauer, G. C., "Heat Transfer in Packed and Fluidized Beds by the Method of Cyclic Temperature Variations," *American Institute of Chemical Engineers Journal*, Vol. 13, 1967, p. 1181.

[18] Bussard, R. W. and De Lauer, R. D., *Fundamentals of Nuclear Flight*, McGraw-Hill Book Co., N.Y., 1965, p. 377.

[19] Eckert, E. R. G. and Drake, R. M., *Heat and Mass Transfer*, McGraw-Hill Book Co., N.Y., 1959, p. 252.